

## An infrared study on CO intercalated in solid C<sub>60</sub>

Iwan Holleman, Gert von Helden, Ad van der Avoird, and Gerard Meijer  
*NSR Center and Research Institute for Materials, University of Nijmegen, Toernooiveld,  
NL-6525 ED Nijmegen, The Netherlands*

(Received 20 August 1998; accepted 20 October 1998)

The infrared (IR) absorbance spectra of CO intercalated in solid C<sub>60</sub> have been measured as a function of temperature. The spectra show a gradual transition from a nearly free rotation of the CO molecules to a situation where their rotational motion is severely hindered. The hindering of the rotational motion of CO caused by the surrounding C<sub>60</sub> molecules is found to be comparable to that observed for CO dissolved in a liquid. Good agreement is found between quantum mechanically calculated spectra and the measured IR spectra. The intermolecular van der Waals vibrations of a CO molecule rattling in the octahedral site of the C<sub>60</sub> lattice have been observed at low temperatures. The IR spectra of CO intercalated in C<sub>70</sub> are measured and compared to those observed for CO intercalated in C<sub>60</sub>. © 1999 American Institute of Physics.  
[S0021-9606(99)00904-6]

### I. INTRODUCTION

The rotational and translational dynamics of small molecules trapped in liquids or solids can be accurately studied using infrared (IR) absorption spectroscopy. Already in the 1960s, it was observed that the IR spectra of the  $\nu_3$  and  $\nu_4$  vibrational bands of methane molecules trapped in the substitutional cavities of rare gas crystals (xenon, krypton and argon) show a fine structure which can be ascribed to the quantized levels of a slightly hindered rotor.<sup>1</sup> More recent high resolution IR measurements on methane trapped in these rare gas matrices have revealed discrete rovibrational transitions, and the observed rotational level spacing is seen to depend on the cavity size, i.e., on the noble gas used.<sup>2</sup> It is well established that in solid hydrogen, the simplest molecular solid, the hydrogen molecules rotate and vibrate nearly freely. Using IR spectroscopy, the pure rotational and rovibrational transitions of a small fraction of ortho-hydrogen trapped in an almost pure para-hydrogen crystal have been observed up to  $\Delta J = 6$  (*W*-branch).<sup>3</sup> In addition, the pure rotational and rovibrational transitions of para-hydrogen have been observed in the solid up to  $\Delta J = 8$  (*Y*-branch),<sup>3,4</sup> and the linewidths of these transitions are seen to approach those of gas phase molecules.<sup>4</sup> Recently, the rotationally resolved IR absorption spectra of SF<sub>6</sub> molecules/dimers and OCS molecules trapped inside superfluid helium-4 clusters have been measured.<sup>5-7</sup> The obtained spectra could be fitted using the Hamiltonian of a free rotor. The resulting rotational constants are considerably smaller (by a factor of 3) than those of the free molecules, however, which is attributed to the interaction of the molecules with the surrounding superfluid.

Recently, we have reported on the rovibrational motion of CO intercalated in the octahedral sites of the face-centered cubic lattice of C<sub>60</sub>. The dynamics of CO in these interstitial sites of the C<sub>60</sub> lattice has been studied using IR spectroscopy, nuclear magnetic resonance (NMR) spectroscopy and theoretical calculations. It has been found that at room temperature the CO molecules are sufficiently free to perform a

rotational motion, while at low temperatures their rotations are hindered.<sup>8</sup> From IR measurements as a function of pressure, i.e., as a function of the size of the interstitial site, a large part of the transition from translationally and rotationally free molecules to rigidly oriented CO molecules has been studied.<sup>9</sup> Here we present detailed IR absorption measurements on CO intercalated in C<sub>60</sub> around both the CO stretch fundamental and the first overtone as a function of temperature. From a band shape analysis, a qualitative picture of the molecular dynamics of CO is obtained, and the results are compared to those obtained for CO dissolved in various liquids. A full quantum mechanical calculation is performed to be able to interpret the observed spectra quantitatively. From an analysis of the isotope shifts of the fundamental transition and the first overtone of the CO stretch vibration, the harmonic frequency and the anharmonicity of CO intercalated in C<sub>60</sub> are obtained. The intermolecular van der Waals modes, which are sensitive probes of the interaction between CO and the surrounding C<sub>60</sub> molecules, have been observed as weak sidebands of the fundamental transition of CO. For comparison, the observed IR spectra of CO intercalated in C<sub>70</sub> are measured as well.

### II. EXPERIMENT

The IR absorption measurements are performed on films of C<sub>60</sub> which have been intercalated with CO gas using high pressure, high-temperature synthesis.<sup>8</sup> For this, high purity C<sub>60</sub> powder (MER Corp., purity  $\geq 99.9\%$ ) is sublimed in high vacuum ( $10^{-6}$  mbar) on a KBr pellet using typically a temperature of 650 °C for a period of one hour. The obtained films of C<sub>60</sub> on KBr usually have a thickness in the range between 15 and 30  $\mu\text{m}$  as determined from IR absorption measurements (*vide infra*). Subsequently, the C<sub>60</sub> film is loaded into a high-pressure vessel (Parr Instrument,  $p \leq 580$  bar and  $T \leq 350$  °C), and it is exposed to typically 240 bar of CO gas (natural abundance, purity 99.0%) at a temperature of 250 °C for a period of a day. After the cooling down of

the high-pressure vessel and the removal of the CO gas, the CO intercalated  $C_{60}$  film is taken out and stored under high vacuum immediately. The CO intercalated  $C_{70}$  films are produced in a similar way using pure  $C_{70}$  powder (MER Corp., purity  $\geq 99\%$ ). Some IR absorption measurements have been performed on  $C_{60}$  films intercalated with 99 atom%  $^{13}C$  enriched  $^{13}CO$  gas. The intercalation of polycrystalline  $C_{60}$  powder with  $^{13}CO$  gas has been described in detail elsewhere.<sup>10</sup> In short, the  $^{13}CO$  gas (Isotec: 11.0 bar·0.45 l with 99 atom%  $^{13}C$ ) is cryo-pumped from the lecture bottle to the high-pressure vessel by cooling the vessel down to liquid nitrogen temperature. After heating of the high-pressure vessel to 250 °C, a  $^{13}CO$  gas pressure of roughly 400 bar is reached. At the end of the high-pressure run, most of the  $^{13}CO$  gas is retrieved by cryo-pumping it back into the lecture bottle.

The IR absorption spectra as a function of temperature are recorded using a Fourier transform infrared (FTIR) absorption spectrometer (Bruker, IFS 66v) and a helium flow cryostat (Oxford, Optistat). The cryostat is placed in the sample chamber of the FTIR spectrometer, and the optical connections to the spectrometer are made through vacuum. The vacuum in the cryostat is maintained by a turbo pump which is backed by a membrane pump, and the pressure is typically on the order of  $10^{-7}$  mbar. The high vacuum in the cryostat is separated by two KBr windows from the vacuum in the FTIR spectrometer, which is pumped by a rotary pump only. The temperature of the sample is monitored on the copper sample mount, and it can be regulated between 4 and 500 K using a temperature controller. The IR spectra are measured using the glowbar light source, the germanium-coated KBr beamsplitter, and the pyro-electric (DTGS) detector of the FTIR spectrometer. The resolution of the spectrometer is either set to 0.2 or to 0.5  $cm^{-1}$ , and the acquisition time per spectrum is on the order of one hour.

In the spectral region centered around the stretch vibration of the CO molecule ( $2000\text{--}2250\text{ cm}^{-1}$ ),  $C_{60}$  exhibits a rich IR absorption spectrum consisting of numerous weak combination modes.<sup>11</sup> This absorption background of  $C_{60}$  is interfering with the spectral structure of the CO molecules in the CO intercalated  $C_{60}$  film, and therefore an accurate correction for this absorption background is required. In order to do so, a series of IR transmission spectra of the CO intercalated  $C_{60}$  film as a function of temperature is measured first. After these measurements the CO intercalated  $C_{60}$  film, while still being mounted in the cryostat, is heated to 200 °C for a few hours to clear the sample of the trapped CO gas. Subsequently, the series of IR transmission spectra is recorded again for the degassed  $C_{60}$  film. The contribution of CO to the IR absorbance spectrum at a certain temperature is obtained by taking the natural logarithm of the ratio of the two corresponding transmission spectra. In the absorbance spectra obtained in this way, those combination modes of  $C_{60}$  that do not shift in frequency upon intercalation with CO are suppressed completely, while even the combination modes with the largest spectral shift upon intercalation with CO (up to 0.5  $cm^{-1}$ ) are still suppressed by approximately a factor of 30.

In the IR spectrum of a  $C_{60}$  film, fringes with an ampli-

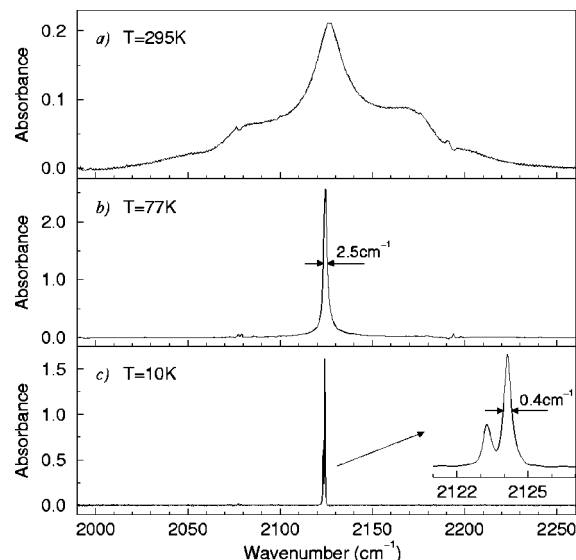


FIG. 1. Measured IR absorption spectra of CO intercalated in  $C_{60}$  as a function of temperature, i.e., (a) 295, (b) 77, and (c) 10 K. The transmission spectra have been measured at a spectral resolution of 0.2  $cm^{-1}$ , and they have been converted into absorbance spectra by taking the natural logarithm (see the experiment section). The spectra shown in (a) and (b) have been measured on the same CO intercalated  $C_{60}$  film with a thickness of 25  $\mu m$ , while the spectrum shown in (c) has been measured on a CO intercalated  $C_{60}$  film with a thickness of approximately 3  $\mu m$  to avoid saturation of the CO absorption.

tude of a few percent of the transmitted intensity are usually clearly visible. These fringes are due to interference between multiple reflections of the IR beam in the  $C_{60}$  film. The period of these fringes in the spectrum is obtained by fitting them to a sine-function. The refractive index of solid  $C_{60}$  as determined from IR measurements has been reported as  $n = 2.00(5)$ .<sup>11</sup> Using this value for the refractive index and the formula for the free spectral range of a Fabry-Perot interferometer, the thickness of a  $C_{60}$  film can be determined from the period of the interference fringes. A residue of these interference fringes is usually still present in the absorbance spectra of CO obtained using the recipe described above. These residual fringes are eliminated by the subtraction of a fit, which is obtained by fitting of these fringes to a sine-function over a large frequency range ( $1800\text{--}2800\text{ cm}^{-1}$ ).

### III. IR ABSORPTION SPECTRA

The IR absorption spectrum of CO intercalated  $C_{60}$  has been measured as a function of temperature, and the spectral structure due to the presence of CO is shown for three different temperatures in Fig. 1. At room temperature, a rather broad ( $100\text{--}200\text{ cm}^{-1}$ ) and smooth IR band is observed centered at 2127  $cm^{-1}$ , approximately 16  $cm^{-1}$  redshifted from the frequency of the stretch vibration of gas phase CO. The sharp features centered at 2078 and 2191  $cm^{-1}$  are caused by combination modes of  $C_{60}$  which are not completely corrected for by the subtraction procedure described in the experiment section. The IR absorption spectrum of gas phase CO at room temperature consists of numerous individual rovibrational transitions (*P*- and *R*-branch), which are spread around the fundamental vibrational frequency of CO (2143

$\text{cm}^{-1}$ ) over a frequency region of roughly  $150 \text{ cm}^{-1}$ . The  $Q$ -branch, which would have given rise to intensity in the center of the rovibrational band, is absent for gas phase CO because of its  $^1\Sigma^+$  electronic ground state.<sup>12</sup> Therefore, the wings of the IR band of CO intercalated in  $\text{C}_{60}$  at room temperature [see Fig. 1(a)], which resemble the envelope of the  $P$ - and  $R$ -branch rotational structure of gas phase CO, are interpreted as the signature of rotational motion of the CO molecules in the octahedral sites, while the intensity in the center of the band of CO, similar to a  $Q$ -branch, is an indication of the amount of hindering of the rotational motion of CO. This interpretation is substantiated by the resemblance of the IR band of CO intercalated in  $\text{C}_{60}$  with the IR spectra of CO dissolved in various chlorinated solvents, and the observed trend in these spectra as a function of solvent interaction.<sup>13</sup>

Upon cooling down, the wings in the IR absorption spectrum of CO intercalated in  $\text{C}_{60}$  gradually disappear and the intensity of the center peak steadily increases. At a temperature of 77 K, a sharp, Lorentzian-like line shape with a full width at half maximum (FWHM) of  $2.5 \text{ cm}^{-1}$  remains [see Fig. 1(b)], indicating that the rotational motion of the CO molecules is severely hindered. The integrated intensities of the IR bands of CO at 295 and 77 K, which are measured using the same CO intercalated  $\text{C}_{60}$  sample, differ only by a fraction of a percent. As a consequence, the CO line at 77 K is one of the strongest features of the entire IR spectrum of CO intercalated  $\text{C}_{60}$ , while the maximum absorption strength of the CO band at room temperature is only comparable to the absorption strengths of the weak  $\text{C}_{60}$  combination modes.

At a temperature of 10 K, the spectral structure of CO is even sharper (a FWHM of  $0.4 \text{ cm}^{-1}$ ), with a concomitant increase of the peak intensity [see Fig. 1(c)], and in order to avoid saturation of the CO line a relatively thin CO intercalated  $\text{C}_{60}$  film ( $d = 3 \mu\text{m}$ ) is used in recording this spectrum. In addition, the resonance of CO at 10 K is split into two components which are separated by  $0.9 \text{ cm}^{-1}$  and have an intensity ratio of approximately 1:2. Apart from this splitting, the spectrum of CO intercalated in  $\text{C}_{60}$  observed at 10 K resembles that of CO in an argon or nitrogen matrix at 15 K,<sup>14</sup> where its rotational motion is completely blocked. The nature of the observed splitting of the CO resonance will be discussed below. In summary, this series of IR spectra of CO as a function of temperature reflects, in agreement with previous measurements,<sup>8</sup> a transition from a nearly free rotational motion of CO at room temperature to a severely hindered motion at low temperature.

The integrated absorbance of the CO band is determined from the IR spectra at 295 and 77 K as  $n\sigma_0d = 13.06(2) \text{ cm}^{-1}$ , where  $n$  is equal to the density of CO,  $\sigma_0$  is the integrated cross section of CO and  $d$  is the thickness of the  $\text{C}_{60}$  film. From the period of the interference fringes [ $\Delta\tilde{\nu} = 101(3) \text{ cm}^{-1}$ ] of the  $\text{C}_{60}$  film used for the measurements at 295 and 77 K, the thickness of this film is determined as  $d = 25(1) \mu\text{m}$ . The product of the CO density times the integrated cross section of CO in this particular sample is thus determined as  $n\sigma_0 = 5.2(2) \times 10^3 \text{ cm}^{-2}$ . Assuming that the integrated cross section of CO intercalated in  $\text{C}_{60}$  is the same as that of gas phase CO [ $\sigma_0 = 9.5(4) \times 10^{-18} \text{ cm}^2 \text{ cm}^{-1}$  (Ref.

15)], the CO density in the CO intercalated  $\text{C}_{60}$  film is found as  $n = 5.5(3) \times 10^{20} \text{ cm}^{-3}$ . At room temperature, the lattice constant of the cubic crystal structure of  $\text{C}_{60}$  is  $a_0 = 14.17 \text{ \AA}$ ,<sup>16</sup> and from this the density of  $\text{C}_{60}$  in the solid is determined as  $1.41 \times 10^{21} \text{ cm}^{-3}$ . As a result, the measurement of the integrated IR absorbance indicates a CO to  $\text{C}_{60}$  ratio of 1:2.6 in the  $\text{C}_{60}$  film, which can be compared to the CO to  $\text{C}_{60}$  ratios varying from 1:9 to 1:1.5 as obtained from  $^{13}\text{C}$  NMR and x-ray measurements on CO intercalated  $\text{C}_{60}$  powder.<sup>10,17</sup>

#### IV. IR BAND SHAPE ANALYSIS

A frequently employed method<sup>13,18–20</sup> to analyze the measured IR spectra of molecules dissolved in liquids is based on the conversion of the IR band shape to an autocorrelation function of the transition dipole moment of the molecule. This method was developed by Gordon in the 1960s.<sup>21</sup> The autocorrelation function contains information on the rotational dynamics of the molecules in the liquid, and it is usually interpreted using rotational diffusion models<sup>18</sup> or molecular dynamics simulations.<sup>20</sup> In order to obtain qualitative insight in the dynamics of the CO molecules in the octahedral sites and to enable a comparison to the dynamics of CO in several liquids, we have applied this method for IR band shape analysis to the spectra of CO intercalated in  $\text{C}_{60}$ . The autocorrelation function of a transition dipole moment is the time evolution of the orientation of this dipole moment [ $\mathbf{u}(t)$ ] projected on its initial orientation [ $\mathbf{u}(0)$ ] and averaged over the ensemble of molecules ( $\langle \rangle$ ). This dipole autocorrelation function  $C(t)$  can be obtained from the IR band shape [ $I(\omega)$ ] via a Fourier transformation:<sup>21</sup>

$$C(t) = \langle \mathbf{u}(0) \cdot \mathbf{u}(t) \rangle = \frac{\int I(\omega) e^{i\omega t} d\omega}{\int I(\omega) d\omega}, \quad (1)$$

$$C(t) \equiv \sum_{n=0}^{\infty} \frac{M(n)}{n!} (it)^n \quad \text{with: } M(n) = \frac{\int \omega^n I(\omega) d\omega}{\int I(\omega) d\omega}. \quad (2)$$

In these equations,  $\omega$  is the angular frequency relative to the center frequency of the IR band shape and  $M(n)$  are the frequency moments of the spectrum. Note that the first few even frequency moments,  $M(2n)$ , describe the short term behavior of the real part of the dipole autocorrelation function. In Fig. 2 the real parts of the autocorrelation functions of the transition dipole moment of CO intercalated in  $\text{C}_{60}$  at 295 and 77 K, obtained from the corresponding experimental IR spectra [see Figs. 1(a) and 1(b)], are shown. For comparison, the autocorrelation functions of CO molecules in the gas phase, calculated from simulated IR spectra of gas phase CO at both temperatures,<sup>12</sup> are also shown in Fig. 2. At both temperatures, the short term behavior ( $< 0.2 \text{ ps}$ ) of the CO molecules in the octahedral sites is rather similar to that of CO in the gas phase. In contrast, the midterm behavior ( $> 1 \text{ ps}$ ) of the CO molecules in the octahedral sites at 77 K is quite different from that of CO in the gas phase; the hindering of the motion of the CO molecules by the surrounding  $\text{C}_{60}$  molecules is reflected by a slow decay of the autocorrelation of the orientation of the CO molecules.

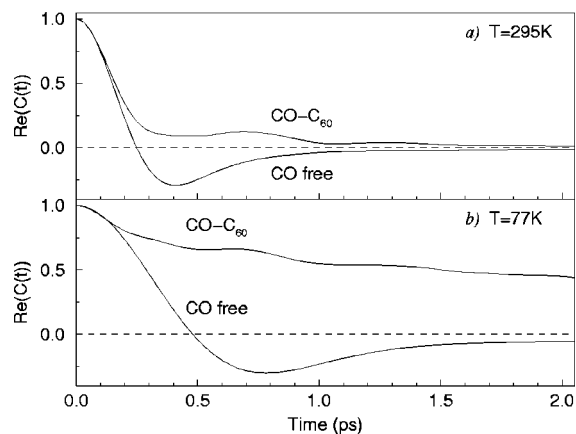


FIG. 2. The real part of the autocorrelation function of the transition dipole moment of CO for CO intercalated in  $C_{60}$  and for CO in the gas phase at 295 (a) and 77 K (b). The dipole autocorrelation functions of CO intercalated in  $C_{60}$  are obtained via Fourier transformation of the experimental IR absorption spectra shown in Figs. 1(a) and 1(b). The dipole autocorrelation functions of gas phase CO are calculated by Fourier transformation of an IR spectrum which is simulated using the rotational constants of CO in the electronic ground state,  $B_0 = 1.9225$  and  $B_1 = 1.9050$   $\text{cm}^{-1}$  (Ref. 12).

For an IR band shape of a linear molecule with a transition dipole moment along its internuclear axis, the second and the fourth frequency moment are, in the classical limit, given by:<sup>21</sup>

$$M(2) = \frac{2kT}{I} = 4BkT, \quad (3)$$

$$M(4) = 2M(2)^2 + 4B^2\langle(\mathbf{OV})^2\rangle. \quad (4)$$

In these equations,  $I$  and  $B$  are the moment of inertia and the rotational constant of the molecule, and  $\langle(\mathbf{OV})^2\rangle$  is the mean-square torque on the molecule due to the surrounding, other molecules. The second moment of the spectrum, and consequently the short time behavior of the dipole autocorrelation function, is independent of the intermolecular forces, and therefore this moment can be used to check the completeness of an IR band shape. The second moments of the IR absorption spectra of CO intercalated in  $C_{60}$  are determined as  $1.52 \times 10^3$   $\text{cm}^{-2}$  at 295 K ( $4BkT = 1570$   $\text{cm}^{-2}$ ) and as  $5.2 \times 10^2$   $\text{cm}^{-2}$  at 77 K ( $4BkT = 410$   $\text{cm}^{-2}$ ). Using the fourth and second moments deduced from the IR absorption spectra, the mean torque acting on the CO molecules due to the surrounding  $C_{60}$  molecules is determined as  $\langle(\mathbf{OV})^2\rangle^{1/2} = 393(25)$   $\text{cm}^{-1}$  (combined value for 295 and 77 K). Interestingly, this result for the mean torque is comparable to the values observed for CO dissolved in liquid argon, several alkanes or various chlorinated solvents, which values are ranging from 195 (liquid Ar) to 493  $\text{cm}^{-1}$  ( $\text{CCl}_4$ ).<sup>18,19,13</sup> In contrast to the voids in a liquid, the sites of the  $C_{60}$  lattice are rigid, symmetrical and uniform, and therefore a full quantum mechanical description of the rovibrational motion of a CO molecule in an octahedral site of the  $C_{60}$  lattice is feasible.

## V. THEORETICAL CALCULATIONS

The IR absorption spectra of CO intercalated in  $C_{60}$  have been calculated at several temperatures using a quantum me-

chanical method. For this, the quantum mechanical model originally developed to describe the rovibrational motion of a CO molecule *inside* a  $C_{60}$  molecule ( $\text{CO}@C_{60}$ )<sup>22</sup> has been modified to be applicable to the motion of CO in an octahedral site of the  $C_{60}$  lattice.<sup>8</sup> In order to understand the set-up of the calculations, some knowledge of the crystal structure of solid  $C_{60}$  is essential. Below the temperature of the orientational ordering transition (240 K), CO intercalated  $C_{60}$ , like pristine  $C_{60}$ , has a simple cubic  $Pa\bar{3}$  crystal structure.<sup>17,23</sup> Both for CO intercalated  $C_{60}$ <sup>17</sup> and for pristine  $C_{60}$ ,<sup>24</sup> two symmetry inequivalent orientations have been found for the  $C_{60}$  molecules in this  $Pa\bar{3}$  crystal structure. These two orientations, denoted  $p$  and  $h$ , correspond to a situation where six electron-poor pentagons of a  $C_{60}$  molecule are facing electron-rich double bonds of 6 of its 12 neighboring  $C_{60}$  molecules ( $p$ -orientation) and to a situation where electron-poor hexagons of a  $C_{60}$  molecule are facing double bonds of its neighbors ( $h$ -orientation).<sup>24</sup> Below the temperature of the glass transition of CO intercalated  $C_{60}$  (84 K), these two orientations of  $C_{60}$  are frozen randomly throughout the CO intercalated  $C_{60}$  lattice in a 12.5:1 ratio of  $p$  to  $h$ .<sup>17,23</sup>

In the calculations, 14 rigid  $C_{60}$  molecules, the six nearest neighbors and the eight next-nearest neighbors of the CO molecule, are positioned on the six faces and the eight corners of the cubic conventional unit cell of the  $Pa\bar{3}$  lattice and oriented according to either the  $p$ - or the  $h$ -orientation. A five-dimensional (5D) van der Waals potential energy surface is modeled by summing all exp-6 atom-atom interactions between a rigid CO molecule and these  $C_{60}$  molecules, as a function of the position of the center of mass and the orientation of the CO molecule. When all  $C_{60}$  molecules are  $p$ -oriented, the symmetry of this potential is  $S_6$ , i.e., it contains a  $C_3$  axis and an inversion point  $i$ . A three-dimensional equipotential cut through this potential has been shown elsewhere.<sup>8</sup> On this potential energy surface, there are a total of eight minima, six of which are symmetry equivalent global minima and two are symmetry equivalent local minima. The two equivalent local minima correspond to a CO molecule aligned or antialigned with the  $C_3$  axis of the potential which coincides with a body diagonal of the cubic unit cell. The six equivalent global minima correspond to a CO molecule approximately (within a few degrees) aligned or antialigned with one of the other body diagonals of the cubic unit cell.

The bound states of the CO molecule in this van der Waals potential are calculated via a discrete variable representation (DVR) of the radial coordinate of the center of mass of CO and an expansion of the angular wave functions in coupled spherical harmonics.<sup>22</sup> This quantum mechanical method includes the angular-radial coupling caused by the hindering potential of the surrounding  $C_{60}$  molecules exactly, and it describes large amplitude vibrations, hindered rotations and tunneling of the CO molecule between equivalent minima. The energy levels and corresponding wave functions of CO are calculated up to a few thousand  $\text{cm}^{-1}$  above the ground state. The energy levels in the first 100  $\text{cm}^{-1}$  above the ground state are shown schematically in Fig. 3(a).

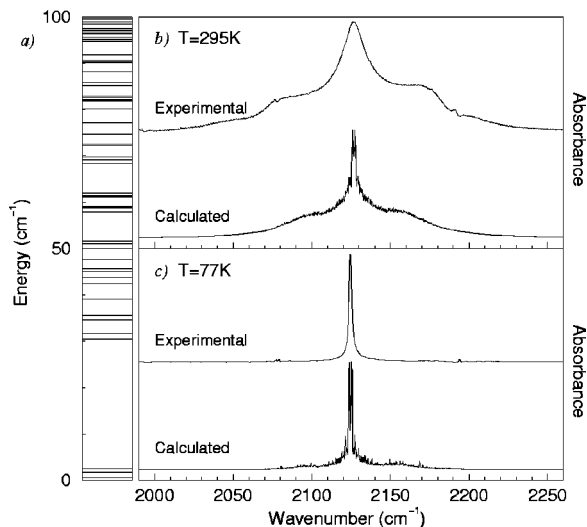


FIG. 3. (a) The calculated energy levels in the first  $100\text{ cm}^{-1}$  above the lowest level in the van der Waals potential of CO intercalated in  $\text{C}_{60}$ . To facilitate a direct comparison of the positions of the calculated energy levels with the infrared spectra the energy is expressed in  $\text{cm}^{-1}$ . A comparison between calculated and experimental IR absorption spectra at a temperature of 295 (b) and of 77 K (c). The calculated stick spectra are convoluted with a Gaussian profile with a full width at half maximum of  $0.25\text{ cm}^{-1}$ , and the center frequencies of the calculated spectra are matched to the experimentally observed values.

The lowest four levels lie within  $3\text{ cm}^{-1}$  of each other and are followed by a gap of about  $30\text{ cm}^{-1}$ . With increasing energy the density of states increases rapidly, and no regularities in the energy level patterns at energies above roughly  $65\text{ cm}^{-1}$  have been found. For the calculation of the IR absorption spectra around the fundamental stretch vibration of CO, the same set of energy levels as calculated for the vibrational ground state ( $v=0$ ) of CO is superimposed on the first excited vibrational level ( $v=1$ ). Subsequently, the transition intensities between the levels at  $v=0$  and those at  $v=1$  are calculated using a dipole function which represents the stretch transition dipole moment of CO. By taking into account the thermal population of the  $v=0$  energy levels and using the calculated transition intensities, the IR absorption spectrum of CO at a certain temperature is synthesized.<sup>22</sup>

In Figs. 3(b) and 3(c) a comparison is made between the calculated and the experimental spectra of CO intercalated in  $\text{C}_{60}$  at temperatures of 295 and 77 K, respectively. Clearly, the agreement between the calculated and the experimental spectra is good. At 295 K, the intensity in the center of the IR band and the shape of the wings on both sides are well reproduced. In addition, the observed disappearance of the wings and the increase of the center intensity upon cooling down to 77 K are reproduced by the calculations as well. The main disagreement between the calculated and the experimental spectra is the absence of the sharp spectral features on the experimental IR band, although the experimental resolution of  $0.2\text{ cm}^{-1}$  should have been sufficient to resolve them. The absence of these features is ascribed to the fact that the calculations neglect the lattice dynamics of the  $\text{C}_{60}$  molecules in the solid, since the  $\text{C}_{60}$  molecules have been fixed. The phonons and librations of the  $\text{C}_{60}$  molecules in the lattice, and, in addition, at room temperature the rapid rotation of the

$\text{C}_{60}$  molecules in the solid,<sup>25</sup> will give rise to temporary deformations of the potential energy surface of CO. Therefore, a superposition of calculated IR spectra for CO in sites with randomly oriented and slightly shifted  $\text{C}_{60}$  molecules has to be performed, which effectively leads to a blurring of the sharp spectral features.

## VI. NATURE OF THE SPLITTING AT 10 K

The lowest four calculated energy levels for CO, of which the middle two are doubly degenerate, are separated, in order of increasing energy, by approximately 0.6, 1.2 and  $0.7\text{ cm}^{-1}$  [see Fig. 3(a)]. The calculated wave functions corresponding to these energy levels are delocalized over the six symmetry equivalent (global) minima in the  $S_6$  potential of CO, indicating the presence of a quantum mechanical tunneling motion between the equivalent minima. At low temperatures, mainly these four energy levels will be populated, and the calculated tunneling motion of CO is expected to result in a splitting of the IR resonance into two sets of lines separated by  $1\text{--}2\text{ cm}^{-1}$  and with an intensity ratio of approximately 1:1.

From the 12.5:1 ratio of *p*- to *h*-oriented  $\text{C}_{60}$  in CO intercalated  $\text{C}_{60}$  below the glass transition, it follows that about two-thirds of the CO molecules are in ‘‘octahedral’’ sites with all six neighboring  $\text{C}_{60}$  molecules *p*-oriented. The potential of CO in such an ‘‘octahedral’’ site has to a good approximation  $S_6$  symmetry. Therefore, the measured splitting of the IR resonance of CO at 10 K into two components, separated by  $0.9\text{ cm}^{-1}$ , could be interpreted as evidence for a tunneling motion of CO between the equivalent minima in this potential.<sup>8</sup> The approximately 50% additional intensity in the high-frequency component should then be attributed to CO in the other one-third of the ‘‘octahedral’’ sites. The latter sites have no symmetry and thus no tunneling motion, and the IR resonance of CO in these sites should then accidentally coincide with the high-frequency component of the tunnel-split resonance of CO in the symmetric sites. If, however, the splitting due to the tunneling motion is less than the linewidth of the individual components ( $0.4\text{ cm}^{-1}$ ) or if the tunneling is ‘‘quenched’’ completely due to coupling with the lattice modes (heat bath),<sup>26</sup> the splitting of the resonance of CO can be interpreted as a result of the presence of CO in at least two different environments having slightly different matrix shifts. Then, the high-frequency component is assigned to CO molecules in the two-thirds of the ‘‘octahedral’’ sites with  $S_6$  symmetry, and the low-frequency component is assigned to CO molecules occupying the other one-third of the ‘‘octahedral’’ sites.

In order to distinguish between these two possibilities, we have measured the splitting of the resonance on the first overtone of CO. For gas phase CO, the absorption strength of the first overtone is about 140 times weaker than that of the fundamental transition.<sup>15</sup> Because of the expected weak coupling between the intermolecular and intramolecular modes, the tunneling motion of CO can to a good approximation be treated independently from the intramolecular stretch vibration of CO, and thus the same set of calculated energy levels can be superimposed on all internal vibrational

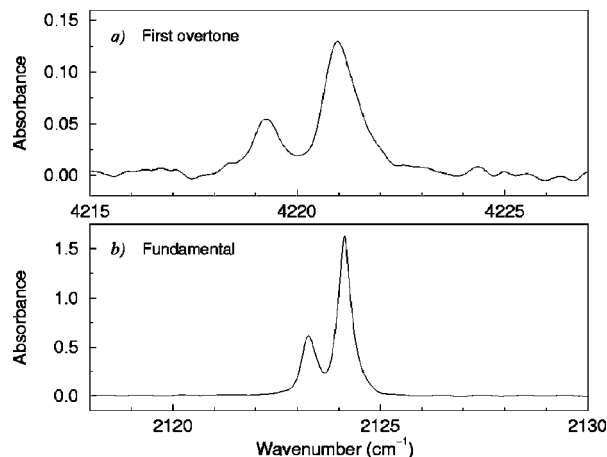


FIG. 4. The measured IR absorbance spectra of CO intercalated in  $C_{60}$  at a temperature of 10 K around the first overtone of CO (a) and around the fundamental transition of CO (b). The CO intercalated  $C_{60}$  film used for the measurement around the first overtone was about a factor of ten thicker than the one used for the measurement around the fundamental transition. The transmission spectra have been measured at an experimental resolution of  $0.2 \text{ cm}^{-1}$ , and they have been converted into absorbance spectra by taking the natural logarithm.

levels of CO ( $v=0,1,2, \dots$ ). Therefore, the splitting due to the tunneling of CO is to a good approximation expected to be independent of the nature of the internal vibrational transition of CO, i.e., fundamental or overtone, on top of which it is observed. On the other hand, if the splitting of the resonance is due to CO occupying different sites, the two observed components are split because they have slightly different vibrational frequencies, and the splitting is expected to double in going from the fundamental to the first overtone of CO.

In Fig. 4, the IR absorption spectrum of CO intercalated in  $C_{60}$  at 10 K measured around the first overtone of CO (a) is shown together with that around the fundamental transition of CO (b). Note that the width of the horizontal scale is exactly the same for Figs. 4(a) and 4(b). It is evident when comparing the two spectra that the splitting is not constant, and that it actually doubles in going from the fundamental to the first overtone. It is detailed below that the positions of the high-frequency and low-frequency components of the fundamental and first overtone of the CO resonance can be described perfectly for all observed isotopes of CO assuming two slightly different independent vibrational frequencies. The splitting due to a tunneling motion would be extremely sensitive to the mass of CO. Therefore, it is concluded that splitting of the resonance originates from the presence of CO in different ‘‘octahedral’’ sites, and that the splitting due to a possible tunneling of CO is either less than  $0.4 \text{ cm}^{-1}$ , or that the tunneling is ‘‘quenched.’’ Both the librations and the phonons of the  $C_{60}$  molecules in the lattice give rise to deformations which could quench the tunneling of CO. From neutron scattering experiments on pristine  $C_{60}$  samples, the librational motion of the  $C_{60}$  molecules in the lattice at zero temperature is expected to still have an amplitude of about two degrees.<sup>27</sup> To examine the influence of these librations of  $C_{60}$  on the tunneling motion of CO, we have performed a calculation for a CO molecule in an octahedral site for which

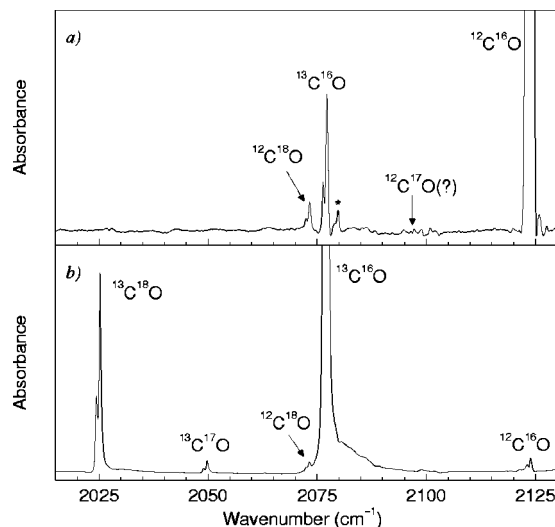


FIG. 5. The IR absorbance spectra of a  $C_{60}$  film intercalated with natural abundance CO gas (a) and a  $C_{60}$  film intercalated with 99 atom%  $^{13}\text{C}$  enriched  $^{13}\text{CO}$  gas (b). Both spectra have been measured at a temperature of 4 K and at a spectral resolution of  $0.2 \text{ cm}^{-1}$ . The different isotopes of CO from which the observed resonances originate have been indicated. The spectral feature marked with an asterisk (\*) is a residue of the  $C_{60}$  combination mode at  $2078 \text{ cm}^{-1}$ .

the  $S_6$  symmetry has been destroyed by rotating one neighboring  $C_{60}$  molecule through two degrees about a specific  $C_3$  axis of  $C_{60}$  away from the  $p$ -orientation. It turns out that this is sufficient to completely localize the wave functions corresponding to the lowest energy levels in the minima, and, as a consequence, to quench the tunneling motion of CO. From recent nuclear magnetic resonance (NMR) measurements on CO intercalated  $C_{60}$  at low temperature, an upper limit of the tunnel rate of CO of only 1.5 kHz is deduced,<sup>10</sup> giving support to the conclusion that the splitting of the IR resonance of CO is due to CO occupying different ‘‘octahedral’’ sites and not to tunneling of CO as concluded previously.<sup>8</sup>

## VII. ISOTOPE SHIFTS

Figure 5(a) shows an IR absorption spectrum measured at 4 K of a thick  $C_{60}$  film intercalated with natural abundance CO gas, and the spectrum is zoomed in on the spectral region where the resonances of the isotopes of CO are expected. Apart from the heavily saturated resonance of  $^{12}\text{C}^{16}\text{O}$  and the spectral feature marked with an asterisk, which is a residue of a combination band of  $C_{60}$ , only two other spectral structures are evident. These spectral structures are identified with the resonances of  $^{13}\text{C}^{16}\text{O}$  and  $^{12}\text{C}^{18}\text{O}$  intercalated in  $C_{60}$ . The natural abundances of  $^{13}\text{C}$  and  $^{18}\text{O}$  are 1.1% and 0.20%, respectively, and thus spectral features related to CO that are roughly a factor of thousand weaker than the fundamental transition can be identified readily using the subtraction procedure of the  $C_{60}$  background as described in the experiment section. An IR absorption spectrum of a thick  $C_{60}$  film intercalated with 99 atom%  $^{13}\text{C}$  enriched  $^{13}\text{CO}$  gas measured at 4 K is shown in Fig. 5(b). The intensity of the resonance of  $^{13}\text{C}^{18}\text{O}$  is about 10% of that of  $^{13}\text{C}^{16}\text{O}$ , and even the reso-

TABLE I. The experimental frequencies of the fundamental transition ( $\tilde{\nu}_{01}$ ) and first overtone ( $\tilde{\nu}_{02}$ ) of the high-frequency ( $h$ ) and low-frequency ( $l$ ) components of the split resonance of CO intercalated in  $C_{60}$  at  $T=4$  K for the different isotopes of CO. The value between parentheses is the experimental error in the last digit. The fitted frequencies of the fundamental transitions [ $\tilde{\nu}_{01}$  (fit)] and the first overtones [ $\tilde{\nu}_{02}$  (fit)] are listed as well. The corresponding harmonic frequencies and anharmonicities for the high-frequency (low-frequency) components, which are scaled to  $^{12}C^{16}O$ , are  $\tilde{\omega}_e(h)=2150.78(8)$   $cm^{-1}$  and  $\tilde{\omega}_e x_e(h)=13.44(3)$   $cm^{-1}$  [ $\tilde{\omega}_e(l)=2149.85(8)$   $cm^{-1}$  and  $\tilde{\omega}_e x_e(l)=13.41(4)$   $cm^{-1}$ ].

Isotope	$\tilde{\nu}_{01}$ ( $cm^{-1}$ )	$\tilde{\nu}_{01}$ (fit) ( $cm^{-1}$ )	$\tilde{\nu}_{02}$ ( $cm^{-1}$ )	$\tilde{\nu}_{02}$ (fit) ( $cm^{-1}$ )
$^{12}C^{16}O(h)$	2123.9(1)	2123.90	4221.0(1)	4220.91
$(l)$	2123.0(1)	2123.04	4219.3(1)	4219.26
$^{12}C^{17}O(h)$		2097.17		4168.14
$(l)$		2096.32		4166.51
$^{13}C^{16}O(h)$	2077.2(1)	2077.14	4128.5(1)	4128.58
$(l)$	2076.3(1)	2076.30	4126.9(2)	4126.96
$^{12}C^{18}O(h)$	2073.2(1)	2073.22		4120.85
$(l)$	2072.4(1)	2072.38		4119.23
$^{13}C^{17}O(h)$	2049.8(1)	2049.78		4074.55
$(l)$	2049.0(1)	2048.95		4072.94
$^{13}C^{18}O(h)$	2025.2(1)	2025.25	4026.0(2)	4026.09
$(l)$	2024.4(1)	2024.43	4024.4(2)	4024.50

nance of  $^{13}C^{17}O$  has appreciable intensity. Obviously, the  $^{13}CO$  gas that we used is actually enriched also in the heavy isotopes of oxygen.

In Table I, the experimentally obtained frequencies of the fundamental transition ( $\tilde{\nu}_{01}$ ) and first overtone ( $\tilde{\nu}_{02}$ ) of the resonance of CO intercalated in  $C_{60}$  at 4 K are listed for different isotopes of CO. The frequencies of both the high-frequency ( $h$ ) and the low-frequency ( $l$ ) components of the split resonance of CO are tabulated. The high-frequency components of both the fundamental and the first overtone of CO for the different isotopes have been fitted to the transitions of an anharmonic oscillator with a harmonic frequency  $\omega_e(h)$  and an anharmonicity  $\omega_e x_e(h)$ , and the low-frequency components are fitted separately but similarly to  $\omega_e(l)$  and  $\omega_e x_e(l)$ . The transition frequencies of the different isotopes are calculated by scaling the harmonic frequency and the anharmonicity with the reduced mass of CO ( $\mu$ ) according to  $\omega_e \propto 1/\sqrt{\mu}$  and  $\omega_e x_e \propto 1/\mu$ .<sup>28</sup> In this way, the harmonic frequency and the anharmonicity of the high-frequency (low-frequency) component are determined from eight different experimental frequencies. The fitted frequencies of the fundamental transitions  $\tilde{\nu}_{01}(fit)$  and the first overtones  $\tilde{\nu}_{02}(fit)$  are listed in Table I as well, and they match the experimental values very well. The resulting harmonic frequencies and anharmonicities, which are scaled to  $^{12}C^{16}O$ , are  $\tilde{\omega}_e(h)=2150.78(8)$  and  $\tilde{\omega}_e x_e(h)=13.44(3)$   $cm^{-1}$  for the high-frequency component and  $\tilde{\omega}_e(l)=2149.85(8)$  and  $\tilde{\omega}_e x_e(l)=13.41(4)$   $cm^{-1}$  for the low-frequency component. These values can be compared to those of gas phase CO in its electronic ground state, which are  $\tilde{\omega}_e=2169.814$  and  $\tilde{\omega}_e x_e=13.288$   $cm^{-1}$ .<sup>12</sup> Thus, the harmonic frequencies are redshifted by 19–20  $cm^{-1}$  and the anharmonicities are hardly changed upon intercalation of CO

in the  $C_{60}$  lattice. Redshifts of 5–10  $cm^{-1}$  of the fundamental vibration of CO have been observed for CO trapped in solid argon and nitrogen matrices at 15 K.<sup>14</sup> It is observed that the redshift of the fundamental transition of CO intercalated in  $C_{60}$  decreases slightly with increasing temperature, at a rate of approximately 1  $cm^{-1}/100$  K.

### VIII. VAN DER WAALS MODES

At low temperatures, the rotational motion of a CO molecule in an octahedral site is severely hindered by the surrounding  $C_{60}$  molecules. As a result, the motion of the CO molecule changes from a more or less free rotation to a libration about an equilibrium orientation of the molecule in the octahedral site, coupled with the translational vibrations. The eigenfrequencies of these intermolecular vibrations of CO are a very sensitive measure of the van der Waals potential energy surface for the interaction between CO and the surrounding  $C_{60}$  molecules. Five fundamental van der Waals modes are expected for a CO molecule located in a minimum of an octahedral site: two librational and three translational modes. We have pursued the observation of these so-called van der Waals modes as (weak) sidebands of the intramolecular fundamental vibration of CO. In the IR absorption spectrum of the thick CO intercalated  $C_{60}$  film at 4 K shown in Fig. 5(a), a set of spectral features can be identified between 50 and 115  $cm^{-1}$  blue shifted from the fundamental transition of  $^{12}C^{16}O$ . The absorption strengths of these spectral features are roughly equal to those of the residue of the  $C_{60}$  combination band marked with an asterisk in Fig. 5(a). Several of these spectral features are interesting because of their striking temperature dependence: they steadily broaden and eventually are washed out in raising the temperature from 4 to about 70 K. Such a strong temperature dependence is not anticipated for the intramolecular combination bands of  $C_{60}$  in this temperature region, because of the rigid molecular structure of the  $C_{60}$  molecule and the fixed orientation of  $C_{60}$  in the lattice at these low temperatures.

Figure 6 shows a series of the temperature dependent spectral features on the blue side of the fundamental transition of  $^{12}C^{16}O$ . Instead of using a spectrum of the degassed  $C_{60}$  film at the corresponding temperature as the reference, a spectrum of the CO intercalated  $C_{60}$  film at a temperature of 70 K has been used to correct for the  $C_{60}$  background in obtaining the spectra shown in this figure. The heavily saturated fundamental transition of  $^{12}C^{16}O$  at 2124  $cm^{-1}$  is not shown in the spectra. The wiggles marked with an asterisk are the residues of the combination band of  $C_{60}$  at 2191  $cm^{-1}$ , which still are not completely corrected for. To check if these spectral features are related to CO, we have measured the same series of spectra as a function of temperature on a  $C_{60}$  film intercalated with 99 atom%  $^{13}C$  enriched  $^{13}CO$ . In Fig. 7 a comparison is made between the spectral structure observed at 4 K on the blue side of the fundamental transition of  $^{13}C^{16}O$  and of  $^{12}C^{16}O$ . The frequency scale is taken relative to the frequency of the high-frequency component of the fundamental transition of the corresponding isotope of CO. Although the absolute frequency scales of the spectra of  $^{13}C^{16}O$  and  $^{12}C^{16}O$  differ by 46.7  $cm^{-1}$  (see Table I)—

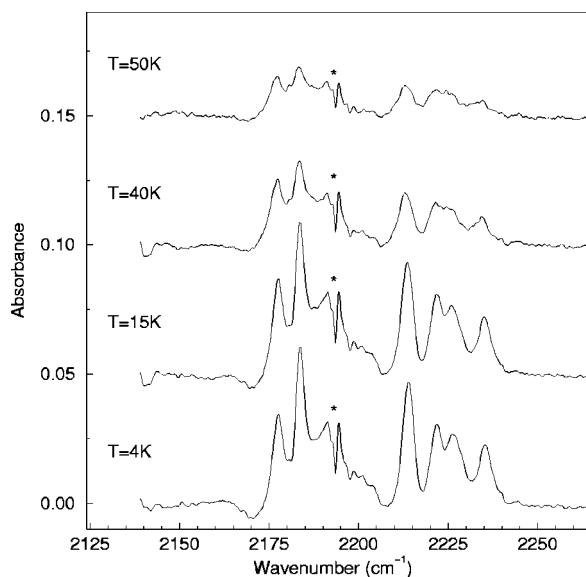


FIG. 6. The measured van der Waals modes of  $^{12}\text{C}^{16}\text{O}$  intercalated in  $\text{C}_{60}$  as a function of temperature, observed as sidebands of the fundamental stretch vibration of  $^{12}\text{C}^{16}\text{O}$ . All spectra (4–50 K) are corrected for the temperature independent  $\text{C}_{60}$  background using a spectrum of CO intercalated  $\text{C}_{60}$  measured at 70 K as the reference, and they are converted into absorbance spectra by taking the natural logarithm. The spectra are recorded using a spectral resolution of  $0.5\text{ cm}^{-1}$ . The wiggles marked with an asterisk (\*) are residues of the combination band of  $\text{C}_{60}$  at  $2191\text{ cm}^{-1}$  which are not completely corrected for.

notice, for instance, the shift of the disturbing  $\text{C}_{60}$  combination mode (\*)—the sideband structures of the fundamental peaks of two isotopes of CO correspond almost perfectly. In addition, it is observed that the sideband structure of  $^{13}\text{C}^{16}\text{O}$  is slightly redshifted with respect to that of  $^{12}\text{C}^{16}\text{O}$ . The observed temperature dependence of this structure is to be an-

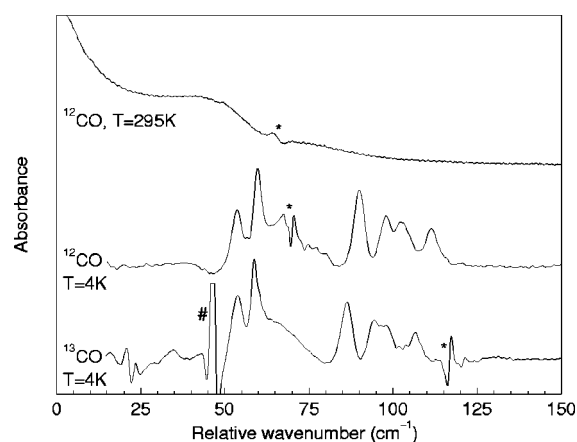


FIG. 7. A comparison between the van der Waals modes of  $^{12}\text{C}^{16}\text{O}$  and those of  $^{13}\text{C}^{16}\text{O}$  intercalated in  $\text{C}_{60}$ , measured as sidebands of the fundamental stretch of CO at a temperature of 4 K. In addition, the wing of the room temperature spectrum of CO intercalated  $\text{C}_{60}$  containing CO in natural abundance is shown. The frequency scale is taken relative to the fundamental transition of CO, i.e., the frequency of the high-frequency component of the resonance of the corresponding isotope of CO (see Table I) is subtracted. The wiggles marked with an asterisk (\*) are residues of a combination band of  $\text{C}_{60}$  which are not completely corrected for. The peak in the spectrum of  $^{13}\text{C}^{16}\text{O}$  intercalated in  $\text{C}_{60}$  marked with a # is the fundamental transition of  $^{12}\text{C}^{16}\text{O}$ , present in the sample as an ‘‘impurity’’ at the 1% level.

TABLE II. The frequency relative to the high-frequency component ( $\tilde{\nu}_{\text{vdw}}$ ), the FWHM ( $\Delta\tilde{\nu}_{\text{vdw}}$ ) and the integrated intensity (Int.) of the van der Waals modes of  $^{12}\text{C}^{16}\text{O}$  and  $^{13}\text{C}^{16}\text{O}$  intercalated in  $\text{C}_{60}$  are listed. The values have been obtained by fitting of the van der Waals sidebands measured at 4 K to a set of Gaussian line shapes. In the last column, the ratio of the frequencies of the van der Waals modes of  $^{13}\text{C}^{16}\text{O}$  and  $^{12}\text{C}^{16}\text{O}$  [ $R(\tilde{\nu}_{\text{vdw}})$ ] is given. The value of  $R(\tilde{\nu}_{\text{vdw}})$  marked with # is too high due to a shift of the lowest van der Waals mode of  $^{13}\text{C}^{16}\text{O}$  caused by an interference with the fundamental transition of  $^{12}\text{C}^{16}\text{O}$ .

$^{12}\text{C}^{16}\text{O}$			$^{13}\text{C}^{16}\text{O}$			$R(\tilde{\nu}_{\text{vdw}})$
$\tilde{\nu}_{\text{vdw}}$ ( $\text{cm}^{-1}$ )	$\Delta\tilde{\nu}_{\text{vdw}}$ ( $\text{cm}^{-1}$ )	Int. (a.u.)	$\tilde{\nu}_{\text{vdw}}$ ( $\text{cm}^{-1}$ )	$\Delta\tilde{\nu}_{\text{vdw}}$ ( $\text{cm}^{-1}$ )	Int. (a.u.)	
53.6(4)	3.4(4)	0.89(5)	53.7(4)	3.5(6)	1.0(8)	1.00(1)#
59.7(3)	2.6(3)	1.00	58.9(3)	3.0(3)	1.00	0.987(7)
66(2)	1.6(3)	3.8(5)	65.0(2)	13(2)	2.7(3)	0.98(4)
90.0(4)	3.7(3)	1.5(1)	86.3(4)	3.7(3)	1.1(1)	0.959(7)
97.5(5)	3.7(5)	0.88(6)	93.8(4)	2.9(8)	0.34(7)	0.962(7)
102.8(6)	5.9(6)	1.4(1)	97.5(7)	6.5(8)	1.1(2)	0.95(1)
111.5(5)	4.8(5)	0.92(6)	106.4(5)	4.5(6)	0.56(4)	0.954(7)

anticipated when it originates from the van der Waals modes of CO intercalated in  $\text{C}_{60}$ . In this temperature region, the librational motion of the  $\text{C}_{60}$  molecules, which has a frequency of about  $22\text{ cm}^{-1}$ ,<sup>27</sup> and the phonons of the  $\text{C}_{60}$  lattice, which have a maximum frequency of about  $55\text{ cm}^{-1}$ ,<sup>29</sup> become thermally activated, and lead to an increase of the temporary deformations of the potential energy surface of CO with increasing temperature. Due to the extreme sensitivity of the frequencies of the van der Waals modes to the potential energy surface of CO, the van der Waals modes of CO are broadened and readily washed out with increasing temperature. It is concluded, therefore, that the observed temperature dependent spectral features on the blue side of the fundamental transition of CO are the sought-after van der Waals modes of CO intercalated in  $\text{C}_{60}$  indeed.

By comparing the spectra of the van der Waals sidebands of  $^{12}\text{C}^{16}\text{O}$  and of  $^{13}\text{C}^{16}\text{O}$  as shown in Fig. 7, six discrete van der Waals modes and a relatively broad band in the gap between the two groups of modes can be identified. These six modes and the broad band as observed for both isotopes have been fitted to a set of Gaussian line shapes, and the results are listed in Table II. The FWHM of the six discrete van der Waals modes range from about  $2.5$  to  $6.5\text{ cm}^{-1}$ , which is roughly a factor of ten larger than the width of the fundamental transition of CO at 10 K [see Fig. 1(c)]. This difference in linewidth is ascribed to the broadening of the van der Waals modes due to coupling with the librations and phonons of the  $\text{C}_{60}$  molecules in the lattice. It has been detailed above that the CO molecules are distributed over at least two different kinds of ‘‘octahedral’’ sites at low temperatures. About two-thirds of the CO molecules occupy ‘‘octahedral’’ sites with  $S_6$  symmetry where all six global minima are symmetry equivalent, while the other one-third of the CO molecules are in sites without any symmetry ( $C_1$ ) where all eight minima are inequivalent. From a calculation of the van der Waals potential energy surface for CO occupying the ‘‘octahedral’’ site with  $C_1$  symmetry, it is found that the energies of the four lowest minima are within about



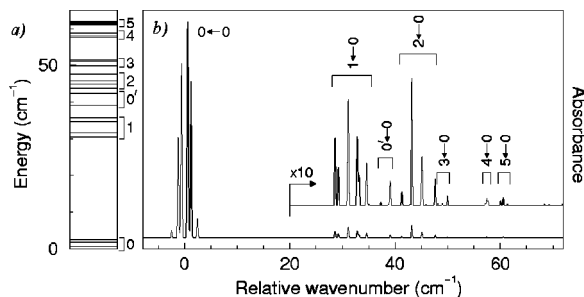


FIG. 8. (a) The calculated energy levels in the first  $65 \text{ cm}^{-1}$  above the ground state. To facilitate a direct comparison of the positions of the calculated energy levels with the infrared spectra the energy is expressed in  $\text{cm}^{-1}$ . The energy levels have been grouped in six quadruplets, of which two levels are doubly degenerate, and one doublet as indicated by the labels in the figure. (b) The calculated IR absorption spectrum of CO intercalated  $\text{C}_{60}$  at a temperature of 4 K. The calculated stick spectrum is convoluted with a Gaussian with a FWHM of  $0.25 \text{ cm}^{-1}$ , and the frequency scale is taken relative to the fundamental vibrational transition of CO. The inset shows the van der Waals sidebands of the fundamental transition on an expanded vertical scale, with the transitions to the different groups of energy levels marked as such.

$8 \text{ cm}^{-1}$ , suggesting that these four inequivalent minima of the  $C_1$  site will still have considerable population at low temperatures. Taking into account the sensitivity of the van der Waals modes to the shape of a minimum, it is likely that the broad band originates from CO in the sites without any symmetry, where a distribution of different van der Waals frequencies is expected, and that the six discrete van der Waals modes belong to CO in the sites having  $S_6$  symmetry.

In Fig. 8 the quantum mechanically calculated IR absorption spectrum of CO in the “octahedral” site with  $S_6$  symmetry at 4 K (b) is shown together with the calculated energy levels in the first  $65 \text{ cm}^{-1}$  above the ground state (a). The inset in Fig. 8(b) shows the calculated van der Waals sidebands on an expanded vertical scale revealing a set of sideband transitions between 25 and  $70 \text{ cm}^{-1}$  blue shifted from the fundamental transition. In the calculation, the van der Waals modes are split due to the tunneling motion of CO which is inherent in the calculation and cannot be “switched off.” Using their frequency, their symmetry label, their isotope shift and the expectation values of a few different operators over their wave function, the lowest 26 energy levels have been grouped in six quadruplets and one doublet as schematically indicated in Fig. 8(a). The quadruplet marked with 0 and the doublet marked with  $0'$  correspond to the lowest energy levels in the six global minima and the two local minima, respectively, while the quadruplets marked with 1–5 correspond to the tunnel-split levels of the five fundamental van der Waals modes in the six global minima. In the calculated IR spectrum of Fig. 8(b), the sideband transitions to the different groups of energy levels are marked. Only the two lowest van der Waals modes have considerable intensity in the calculated IR spectrum. Since the transition dipole moment function used in the calculations depends only on the angles  $\theta$  and  $\phi$  which determine the orientation of CO, and not on its center of mass position, see Eq. (33) in Ref. 22, it follows that only the librational modes have IR intensity. Therefore, these two lowest van der Waals modes are identified with the two librational modes of CO. The

weak intensity of the other three modes is induced by some mixing of the translational and librational motions. By averaging over the energy levels in the quadruplets, the calculated frequencies of the van der Waals modes of CO in a global minimum are determined as 32, 44, 50, 57 and  $60 \text{ cm}^{-1}$ , and their isotope shift ratios ( $\tilde{\nu}[^{13}\text{CO}]/\tilde{\nu}[^{12}\text{CO}]$ ) are determined as 0.991, 0.986, 0.979, 0.973 and 0.971, respectively.

Both the frequencies and the isotope shift ratios of the experimentally observed van der Waals modes indicate that the six discrete modes fall into two groups, two low-frequency modes ( $50\text{--}60 \text{ cm}^{-1}$ ) and four high-frequency modes ( $80\text{--}115 \text{ cm}^{-1}$ ). From a comparison with the calculated spectrum, the two lowest frequency modes are tentatively assigned as the fundamental librational modes. For the other four modes, two possible assignments remain. First, they may, in part, be due to fundamental translational modes that can acquire intensity through a transition dipole moment induced by the interaction between CO and the surrounding  $\text{C}_{60}$  molecules, an effect that is not accounted for in the calculations. Second, they may have to be assigned to van der Waals modes that correspond with higher bands, overtone or combination bands, in the harmonic limit, even though these modes do not appear with such a high intensity in the calculated spectra. The intensity of these modes will be very sensitive to the shape of the potential energy surface used, and our model potential is perhaps not sufficiently accurate to describe them properly. A further theoretical analysis of these van der Waals modes of CO intercalated in  $\text{C}_{60}$ , using an empirically optimized potential energy surface and taking the effect of the heat bath of  $\text{C}_{60}$  on the tunneling motion of CO into account, will be needed to provide an unambiguous assignment.

## IX. CO INTERCALATED IN $\text{C}_{70}$

The IR absorption spectra of natural abundance CO intercalated in  $\text{C}_{70}$  have been measured, and the spectral structure due to the presence of CO is shown for two different temperatures in Fig. 9. At room temperature, the IR band of CO intercalated in  $\text{C}_{70}$  and that of CO intercalated in  $\text{C}_{60}$  [see Fig. 1(a)] are evidently rather similar. There are a few subtle differences between the IR bands, however. When comparing the IR band of CO intercalated in  $\text{C}_{70}$  in detail to that of CO intercalated in  $\text{C}_{60}$ , it turns out that the intensity in the center of the band is somewhat less, that the intensity difference between the high-frequency and low-frequency wing is more pronounced, and that the wings are less structured. The integrated absorbance of the IR band of CO intercalated in  $\text{C}_{70}$  at room temperature [Fig. 9(a)] is determined as  $n\sigma_0d = 7.34(2) \text{ cm}^{-1}$ . From the period of the interference fringes [ $\Delta\tilde{\nu} = 546(4) \text{ cm}^{-1}$ ] of the degassed  $\text{C}_{70}$  film and assuming that the refractive index of  $\text{C}_{70}$  is equal to that of  $\text{C}_{60}$ , the thickness of the  $\text{C}_{70}$  film is determined as  $d = 4.6 \mu\text{m}$ . Assuming again that the integrated cross section of CO remains unchanged upon intercalation, the CO density in the CO intercalated  $\text{C}_{70}$  film is found as  $n = 1.7 \times 10^{21} \text{ cm}^{-3}$ . This density of CO in the  $\text{C}_{70}$  film is about a factor of three higher than that obtained for CO intercalated in  $\text{C}_{60}$ , which implies

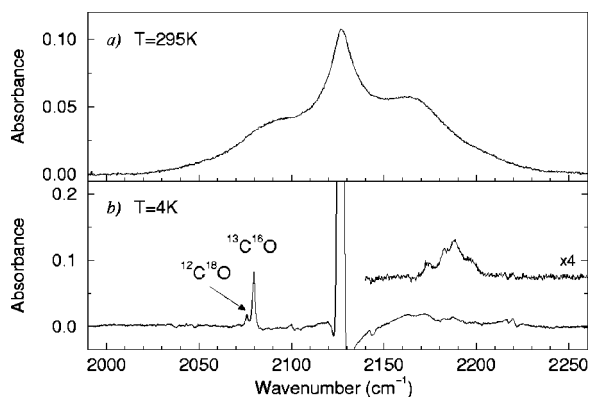


FIG. 9. The additional spectral structure due to natural abundance CO which is intercalated in  $C_{70}$  recorded at room temperature (a) and at 4 K (b). The inset in (b) shows, on an expanded vertical scale, the temperature dependent sideband structure of the fundamental transition of CO intercalated in  $C_{70}$  measured at 4 K, which has been obtained by using a spectrum of CO intercalated in  $C_{70}$  measured at 70 K as the reference. The transmission spectra have been recorded at a spectral resolution of  $0.2 \text{ cm}^{-1}$ , and they have been converted into absorbance spectra by taking the natural logarithm.

an approximate 1:1 ratio of CO to  $C_{70}$  in the  $C_{70}$  film. At the high temperature ( $200^\circ\text{C}$ ) used to intercalate the CO gas into the  $C_{70}$  film, the crystal structure of  $C_{70}$  is face-centered cubic (fcc), where the  $C_{70}$  molecules in the lattice are orientationally disordered.<sup>30</sup> The lattice constant of this fcc phase of  $C_{70}$  is  $a_0 = 15.0 \text{ \AA}$ ,<sup>30,31</sup> which is substantially larger than that of the fcc phase of  $C_{60}$  [ $14.2 \text{ \AA}$ ].<sup>16</sup> As a result of this larger lattice constant, both the octahedral sites and the diameter of the channels between these sites are larger. Obviously, this facilitates the intercalation process significantly. By comparing the integrated absorbance of the room temperature spectrum of CO intercalated in  $C_{70}$  shown in Fig. 9(a) to that determined from a spectrum which is measured three days later, it follows that CO leaks out of the  $C_{70}$  lattice at a rate of about 35% per day at room temperature. This CO loss rate is approximately an order of magnitude higher than that observed for CO intercalated in  $C_{60}$ .<sup>8</sup>

In Fig. 9(b), the absorbance spectrum of CO intercalated in  $C_{70}$  at 4 K is shown in the region around the heavily saturated, fundamental transition of  $^{12}\text{C}^{16}\text{O}$ . From the IR bands of the isotopes of CO and that of the first overtone of  $^{12}\text{C}^{16}\text{O}$  (not shown), it is evident that the IR band of CO intercalated in  $C_{70}$  at low temperatures consists of a single resonance. The resonance of  $^{12}\text{C}^{16}\text{O}$  intercalated in  $C_{70}$  is centered at approximately  $2126.4 \text{ cm}^{-1}$ , and it is thus less redshifted from the resonance of gas phase CO than the doublet of  $^{12}\text{C}^{16}\text{O}$  intercalated in  $C_{60}$ . The FWHM of the resonance of CO intercalated in  $C_{70}$  is about four times as large as that of the high-frequency component of the resonance of CO intercalated in  $C_{60}$ . This difference in linewidth is probably due to the presence of several different interstitial sites in the  $C_{70}$  lattice caused by disorder in the stacking of orientationally ordered close packed layers at low temperature.<sup>31</sup> The inset of Fig. 9(b) shows the temperature dependent sideband structure of the fundamental transition of  $^{12}\text{C}^{16}\text{O}$  intercalated in  $C_{70}$  at 4 K. This sideband spectrum has been obtained in a similar way as the spectra of the van der Waals modes of CO intercalated in  $C_{60}$ . The high-frequency van

der Waals modes (between  $2210$  and  $2240 \text{ cm}^{-1}$ ) as observed for CO intercalated in  $C_{60}$  are absent for CO intercalated in  $C_{70}$ . It is evident that the sideband spectrum of CO intercalated in  $C_{70}$  is less structured than that of CO intercalated in  $C_{60}$ , and will be even harder to be interpreted unambiguously.

## X. CONCLUSIONS

The IR absorbance spectra of CO intercalated in  $C_{60}$  have been measured as a function of temperature. The evolution of the IR band of CO as a function of temperature reflects a smooth transition from a situation of nearly free rotation of the CO molecules in the solid to a situation where the rotational motion of CO is severely hindered. An IR band shape analysis indicates that the hindering of CO caused by the surrounding  $C_{60}$  molecules is comparable to that observed for CO dissolved in a liquid. The CO intercalated  $C_{60}$  system allows for a detailed quantum mechanical modeling, and both at room temperature and at  $77 \text{ K}$  a good agreement is found between the calculated and the measured IR spectra. It turns out that the calculated tunneling motion of CO at low temperature is quenched because of coupling to the heat bath, i.e., to the translational and librational motions of the  $C_{60}$  molecules in the lattice. The intermolecular van der Waals vibrations of a CO molecule rattling in an octahedral site of the  $C_{60}$  lattice at low temperatures have been observed as weak sidebands of the fundamental transition of CO. A tentative assignment of these van der Waals modes using theoretical calculations has been discussed. At room temperature the IR spectrum of CO intercalated in  $C_{70}$  is rather similar to that of CO intercalated in  $C_{60}$ , whereas at lower temperatures the sites in the  $C_{70}$  lattice seem less well defined than the sites of the  $C_{60}$  lattice.

## ACKNOWLEDGMENTS

This work is part of the research program of the ‘‘Stichting voor Fundamenteel Onderzoek der Materie (FOM),’’ which is financially supported by the ‘‘Nederlandse Organisatie voor Wetenschappelijk Onderzoek (NWO),’’ and receives direct support by the NWO via PIONIER-Grant No. 030-66-089.

- <sup>1</sup>A. Cabana, G. B. Savitsky, and D. F. Hornig, *J. Chem. Phys.* **39**, 2942 (1963).
- <sup>2</sup>L. H. Jones, S. A. Ekberg, and B. I. Swanson, *J. Chem. Phys.* **85**, 3203 (1986).
- <sup>3</sup>R. A. Steinhoff, B. P. Winnewisser, and M. Winnewisser, *Phys. Rev. Lett.* **73**, 2833 (1994).
- <sup>4</sup>M. Okumura, M.-C. Chan, and T. Oka, *Phys. Rev. Lett.* **62**, 32 (1989).
- <sup>5</sup>M. Hartmann, R. E. Miller, J. P. Toennies, and A. F. Vilesov, *Phys. Rev. Lett.* **75**, 1566 (1995).
- <sup>6</sup>M. Hartmann, R. E. Miller, J. P. Toennies, and A. F. Vilesov, *Science* **272**, 1631 (1996).
- <sup>7</sup>S. Grebenev, J. P. Toennies, and A. F. Vilesov, *Science* **279**, 2083 (1998).
- <sup>8</sup>I. Holleman, G. von Helden, E. H. T. Olthof, P. J. M. van Bentum, R. Engeln, G. H. Nachttegaal, A. P. M. Kentgens, B. H. Meier, A. van der Avoird, and G. Meijer, *Phys. Rev. Lett.* **79**, 1138 (1997).
- <sup>9</sup>I. Holleman, G. von Helden, A. van der Avoird, and G. Meijer, *Phys. Rev. Lett.* **80**, 4899 (1998).

- <sup>10</sup>I. Holleman, P. Robyr, A. P. M. Kentgens, B. H. Meier, and G. Meijer, *J. Am. Chem. Soc.* (in press).
- <sup>11</sup>K.-A. Wang, A. M. Rao, P. C. Eklund, M. S. Dresselhaus, and G. Dresselhaus, *Phys. Rev. B* **48**, 11,375 (1993).
- <sup>12</sup>K. P. Huber and G. Herzberg, *Constants of Diatomic Molecules* (Van Nostrand, New York, 1979).
- <sup>13</sup>S. Baude, A. Idrissi, and G. Turrell, *Can. J. Appl. Spec.* **41**, 60 (1996).
- <sup>14</sup>Y. Ogawara, A. Bruneau, and T. Kimura, *Anal. Chem.* **66**, 4354 (1994).
- <sup>15</sup>L. A. Pugh and K. N. Rao, *Molecular Spectroscopy: Modern Research* (Academic, New York, 1976), Vol. II.
- <sup>16</sup>P. A. Heiney, J. E. Fischer, A. R. McGhie, W. J. Romanow, A. M. Denenstein, J. P. McCauley Jr., and A. B. Smith III, *Phys. Rev. Lett.* **66**, 2911 (1991).
- <sup>17</sup>S. van Smaalen, R. Dinnebier, I. Holleman, G. von Helden, and G. Meijer, *Phys. Rev. B* **57**, 6321 (1998).
- <sup>18</sup>G. Lévi, M. Chalaye, F. Marsault-Herail, and J. P. Marsault, *Mol. Phys.* **24**, 1217 (1972).
- <sup>19</sup>D. Richon, D. Patterson, and G. Turrell, *Chem. Phys.* **24**, 227 (1977).
- <sup>20</sup>L.E. Bowman, B. J. Palmer, B. C. Garrett, J. L. Fulton, C. R. Yonker, D. M. Pfund, and S. L. Wallen, *J. Phys. Chem.* **100**, 18,327 (1996).
- <sup>21</sup>R. G. Gordon, *J. Chem. Phys.* **43**, 1307 (1965).
- <sup>22</sup>E. H. T. Olthof, A. van der Avoird, and P. E. S. Wormer, *J. Chem. Phys.* **104**, 832 (1996).
- <sup>23</sup>S. van Smaalen, R. Dinnebier, W. Schnelle, I. Holleman, G. von Helden, and G. Meijer, *Europhys. Lett.* **43**, 302 (1998).
- <sup>24</sup>W. I. F. David, R. M. Ibberson, T. J. S. Dennis, J. P. Hare, and K. Prassides, *Europhys. Lett.* **18**, 219 (1992).
- <sup>25</sup>R. D. Johnson, C. S. Yannoni, H. C. Dorn, J. R. Salem, and D. S. Bethune, *Science* **255**, 1235 (1992).
- <sup>26</sup>V. A. Benderskii, D. E. Makarov, and C. A. Wight, *Chemical Dynamics at Low Temperatures* (Wiley, New York, 1994).
- <sup>27</sup>J. R. D. Copley, D. A. Neumann, R. L. Cappelletti, and W. A. Kamitakahara, *J. Phys. Chem. Solids* **53**, 1353 (1992).
- <sup>28</sup>G. Herzberg, *Spectra of Diatomic Molecules* (Van Nostrand, New York, 1950), p. 141.
- <sup>29</sup>S. Huant, J. B. Robert, G. Chouteau, P. Bernier, C. Fabre, and A. Rassat, *Phys. Rev. Lett.* **69**, 2666 (1992); S. A. FitzGerald and A. J. Sievers, *ibid.* **70**, 3175 (1993).
- <sup>30</sup>G. B. M. Vaughan, P. A. Heiney, J. E. Fischer, D. E. Luzzi, D. A. Ricketts-Foot, A. R. McGhie, Y. W. Hui, A. L. Smith, D. E. Cox, W. J. Romanow, B. H. Allen, N. Coustel, J. P. McCauley, Jr., and A. B. Smith, III, *Science* **254**, 1350 (1991).
- <sup>31</sup>M. A. Verheijen, H. Meekes, G. Meijer, P. Bennema, J. L. de Boer, S. van Smaalen, G. van Tendeloo, S. Amelinckx, S. Muto, and J. van Landuyt, *Chem. Phys.* **166**, 287 (1992).